

# Plasma Polymerization of Tetrafluoroethylene. II. Capacitive Radio Frequency Discharge

N. MOROSOFF and H. YASUDA,\* *Research Triangle Institute, Research Triangle Park, North Carolina 27709*, and E. S. BRANDT and C. N. REILLEY, *Department of Chemistry, University of North Carolina, Chapel Hill, North Carolina 27514*

## Synopsis

The plasma polymerization of tetrafluoroethylene (TFE) is studied in a capacitively coupled system with internal electrodes using radio frequency (13.56 MHz) power. The emphasis is on identifying conditions that are compatible with continuous coating of plasma polymer on a substrate moving through the center of the interelectrode gap. At high pressure (500 mTorr), deposition of plasma polymer is primarily on the electrodes rather than on a substrate placed midway between electrodes. Glow is observed in only part of the interelectrode gap at low powers and fills the gap only at high power levels. The use of a magnetic field effects barely discernible changes. Low-pressure (below 100 mTorr) operation is more favorable for deposition of a substantial portion of the plasma polymer on a substrate placed midway between electrodes. The plasma polymer deposited at low pressure is characterized by ESCA and deposition rate data and compared to that deposited in an inductively coupled system. The polymers formed in both systems are broadly similar and completely different from conventional poly(TFE). Subtle system-dependent differences are identified. The known susceptibility of fluorine-containing polymers (including plasma polymer) to a high-power plasma has been used as a probe of plasma power density within the interelectrode gap in the capacitively coupled system. Without magnets the most active zone of the plasma is in the center of the interelectrode gap. The use of a magnetic field moves this active zone closer to the electrodes and leads to a more efficient coupling of energy to a polymerizing glow discharge.

## INTRODUCTION

Radio frequency (rf) may be coupled to a glow discharge either inductively, by use of a coil wrapped around the glow discharge tube, or capacitively, by use of two parallel plates, either internal or external to the glow discharge vessel. This investigation deals with a capacitively coupled system employing internal electrodes. Such a system compares advantageously with the inductively coupled system for scale-up to mass production because polymer can be deposited mainly on a substrate placed midway between electrodes. This is an obvious benefit in the continuous plasma polymer coating of films or fibers.

In an inductively coupled glow discharge, a major fraction of the polymer is deposited, unfortunately, on the glass walls of the tubing containing the glow discharge. However, even in the capacitively coupled system, polymer is deposited on the electrodes. The ideal is deposition of plasma polymer only on the substrate, with no deposition on any other surface.

Most studies in the literature have been concerned exclusively with the properties of the deposit on the electrode. In this investigation the rate of plasma

\* Present address: Department of Chemical Engineering, University of Missouri-Rolla, Rolla, Missouri 65401.

polymer deposition has been measured on the electrode and on a substrate placed midway between electrodes, using tetrafluoroethylene (TFE) as the monomer. The study particularly explores conditions in which deposition is minimized on the electrode. For this reason the chemical nature of the polymer formed in a low flow rate [ $F = 2 \text{ cm}^3 \text{ (S.T.P.)}/\text{min}$ ], and low pressure (60 mTorr) plasma has been analyzed by the use of ESCA (electron spectroscopy for chemical analysis). This method combined with the unusual characteristics of TFE plasma polymerization (described below) has yielded information concerning the distribution of power in the interelectrode gap. Somewhat less emphasis has been placed on the characteristics of plasma polymerization at higher flow rates and pressures. A comparison is made of the present results with those obtained for TFE using inductively coupled reactors as well as the capacitively coupled reactor operated at 10 kHz and at 60 Hz.

### Unusual Aspects of TFE Plasma Polymerization

ESCA is particularly well suited for the study of plasma polymerization because it yields information about the elemental makeup of the surface to a depth of a 50 Å or less and is not influenced by the substrate properties. However, it yields little information about the functional groups present in the polymer, except for some special cases where a large enough chemical shift is observed. Thus, little besides information concerning elemental composition can be obtained from an ESCA investigation of the plasma polymerization of hydrocarbons. However, fluorine does cause a large enough chemical shift that the position of the  $C_{1s}$  peak of a carbon bonded to three fluorines ( $CF_3$ ) can be distinguished from that of one bonded to two fluorines ( $CF_2$ ), and both are clearly separated from the normal  $C_{1s}$  peak, i.e., one not bonded to any fluorines.<sup>1</sup> It is clear that the plasma polymerization of tetrafluoroethylene is particularly amenable to study by ESCA.

The plasma polymerization of tetrafluoroethylene (TFE) has been widely studied.<sup>1-7</sup> It has been found to be unusual in that the monomer is sensitive to discharge power.<sup>1-4</sup> Both deposition rate data and ESCA analysis of plasma polymerization in inductively coupled systems demonstrate that fluorine poor polymers are formed when the excited monomer passes through a high power density region of the plasma. Because of the non-negligible atomic weight of fluorine, this fluorine abstraction results in lower deposition rates at very high energy per unit mass of monomer feed.

Deposition rate and ESCA results on blanks placed at various sites in the plasma reactor may therefore be used as a probe of the power density distribution in a given reactor with a glow discharge fed by tetrafluoroethylene.

### Plasma Polymerization of TFE in Inductively Coupled Systems

We may compare results presented here with those obtained in two types of inductively coupled reactors.<sup>1,2</sup> One is the reactor we have used for many years,<sup>8</sup> in which the portion of the reactor inserted into the rf coil is smaller than the main portion of the reactor in which plasma polymer is collected. Monomer influx is directed into the main portion of the reactor, not through the rf coil. Electron bombardment of plasma polymer and substrate is reduced in this way.<sup>9</sup> Active

species are formed mainly under the rf coil and are transported by diffusion to the entire volume of the reactor. Interaction of these nonpolymerizable energy carrying species (e.g., electrons, excited atoms) with the monomer entering the reactor leads to plasma polymerization.<sup>9</sup>

The energy supplied per gram of monomer feed may be given as  $W/FM$ , where  $W$  is the power input,  $F$  is the flow rate, and  $M$  is the molecular weight.  $W_e/FM$ , a measure of the minimum power necessary to maintain full glow in the reactor described above, increases with flow rate (pumping rate constant) for monomers which yield hydrogen gas during the plasma polymerization process.<sup>10</sup> Since the pressure of evolved hydrogen gas increases with monomer flow rate, it is clear that this reflects the power lost as hydrogen is excited and emits radiation (UV or visible). For the case of tetrafluoroethylene,  $W_e/FM$  is  $1.2 \times 10^8$  J/kg.<sup>1,10</sup> The deposition rate begins to decrease because of the above-mentioned fluorine abstraction in this system when  $W/FM$  exceeds  $4.7 \times 10^8$  J/kg.<sup>1,10</sup>

The plasma polymerization of tetrafluoroethylene has also been studied in a straight-tube reactor. Deposition rates and ESCA results were obtained as a function of location upstream from, within, and downstream from the induction coil.<sup>2</sup> It was found that fluorine-poor polymer was formed downstream from the coil even at the relatively low power level of  $1.9 \times 10^7$  J/kg. Fluorine-poor polymer was formed at all locations at  $7.7 \times 10^8$  J/kg.

### Plasma Polymerization in Capacitively Coupled Systems

A capacitively coupled system differs in two respects from those described above. Firstly, the rf field would be expected to be distributed more nearly uniformly over the interelectrode gap than is the case of the reactor volume in an inductively coupled system. Secondly, the flow rate into the plasma is not known as precisely as for the latter. This is because not all monomer feed must drift into the interelectrode gap. On the other hand, the flow into the gap cannot be obtained from the knowledge of the fraction of reactor volume the interelectrode gap represents because the plasma polymerization process acts as a pump.

Moreover, the range of energy per gram of monomer feed that can be used for plasma polymer deposition within the interelectrode gap is limited for an rf glow discharge at low pressure. This is because at low pressure and high powers, rf plasma tends to expand outside the interelectrode gap. In the extreme case glow may be observed everywhere except in the interelectrode gap. This may be avoided by use of a magnetic field to confine the plasma inside the gap, thus making possible higher power densities in the glow discharge. The distribution of glow becomes somewhat less uniform within the gap with such magnetic enhancement. The effect of magnetic enhancement on the tetrafluoroethylene glow discharge and resultant plasma polymer is described below.

Finally, the results presented are to be contrasted with those obtained for plasma polymerization of tetrafluoroethylene using capacitively coupled audio frequency (10 kHz) and ac (60 Hz) glow discharges.<sup>11</sup> The glow discharges treated in this (rf) and the following paper<sup>11</sup> (af and ac) are fundamentally different.<sup>12</sup> The audio frequency (af) and ac discharges are powered by secondary electrons emitted from the electrode and accelerated through a high potential drop. An rf glow discharge is maintained by electrons oscillating between

electrodes and achieving ionizing energies by means of numerous collisions without ever contacting the electrodes.

## EXPERIMENTAL

The apparatus used in this study is illustrated schematically in Figure 1. Two circular aluminum electrodes 14 cm in diameter are placed in a Pyrex glass cross. The glass cross is connected to a vacuum pump by way of a stopcock followed by a liquid nitrogen trap. It is also connected to a differential pressure transducer (the MKS Baratron Pressure Meter) for the purpose of measuring the pressure both with and without a glow discharge.

Magnetic enhancement of the glow discharge was achieved as follows: An iron ring (9.5-cm diameter) is concentrically attached to, but insulated from, the back of each aluminum electrode. A small disk (4.5 cm in diameter) is similarly attached to the back of the electrode. Four permanent horseshoe magnets are placed with north poles on the iron ring and south poles on the small iron disc. The north-south vectors of the magnets are oriented at 90° intervals. In this way a donut-shaped magnetic field is set up projecting into the interelectrode gap, cylindrically symmetrical about an axis passing through the electrode centers. The magnetic field vectors pass out of the electrode near its outer edge into the interelectrode gap, curve in toward the electrode center axis, and turn back toward the electrode, reentering it near its center. A donut-shaped field is thus defined, with the donut "hole" on the electrode center axis. Such a magnetic field tends to prevent escape of electrons (moving between electrodes) outside the interelectrode gap. It also forces electrons to take a convoluted path in oscillating between electrodes. This increases the probability of electron-molecule collisions as compared to the case where no magnetic field is present and electrons may move in a straight line from one electrode to the other. The effect is to concentrate the plasma between electrodes, particularly for low pressures.

The rf power supply is a radio-frequency transmitter, Heathkit Model SX60B. The output is fed into a linear amplifier Heathkit SB-200, having a 500-W capacity. The amplifier output is coupled to the electrodes through a Bendix coupler Model 262, 0.5–225 MHz. The rf power supply operates at 13.56 MHz and delivers continuously variable output power from 0 to 500 W. A tuning circuit, located between the electrodes and the coupler, is used to match the impedance of the discharge vessel and the impedance of the amplifier output. The tuning circuit is adjusted so that the reflected power is maintained at the minimum.

In order to collect polymer at the center of the interelectrode gap, an aluminum foil substrate 8 cm in width was suspended between electrodes as shown in Figure 1. Deposition rates at various locations on the substrate and electrode were obtained by measuring the weight gain of small pieces of aluminum foil (sampling blank) affixed to a given site so that electrical contact was maintained between the site of interest and the sampling blank. This was accomplished by folding the ends of a  $0.5 \times 3$  cm<sup>2</sup> piece of aluminum foil around the ends of a  $0.5 \times 2.2$  cm<sup>2</sup> piece of glass cover slip and affixing the center of the glass cover slip to the electrode or substrate with double-coated scotch tape.

Samples for ESCA analysis were prepared in the same manner and on the same sampling blanks as used for the deposition rate studies. The following spectral

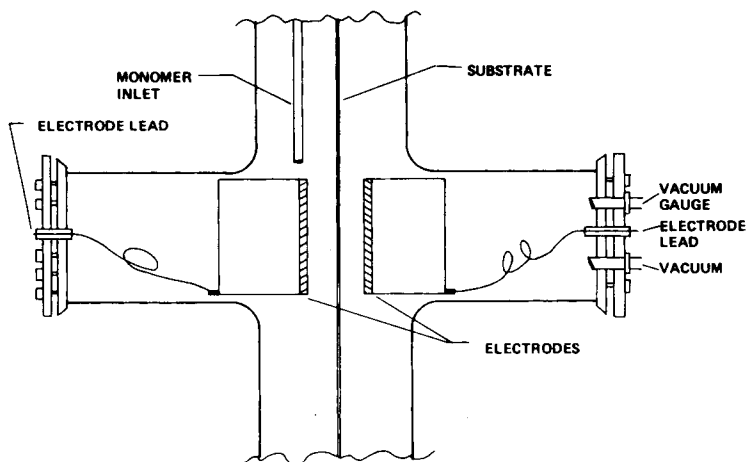


Fig. 1. Schematic representation of the plasma reactor.

lines were obtained from each blank:  $O_{1s}$ ,  $F_{1s}$ ,  $C_{1s}$ , and  $Al_{2s}$  by using a du Pont Model 650 spectrometer with a  $MgK_{\alpha}$  x-ray source and equipped with a micro-computer data acquisition and processing system. Spectra are corrected for charging. Details of the experimental procedure are described elsewhere.<sup>13</sup>

## RESULTS

### Visual Observation of the Glow Discharge

Photographs were taken of glow discharges at a variety of flow rates (influx), applied powers, and pumping rates (efflux), both with and without magnetic enhancement. A qualitative description of all glow patterns observed is given in Table I. The numbers in the "description of glow pattern" column refer to the fraction of the interelectrode gap filled with glow (estimated). Expansion of the glow out of the gap is indicated by 1+.

In the table  $p_M$  is the steady-state flow pressure prior to the initiation of glow discharge and  $p_g$  indicates the pressure reading during the plasma polymerization. Because of the independent control of feed rate and pumping rate, several values of  $p_M$  (and  $p_g$ ) can be achieved for a given flow rate.

Two conclusions can be drawn from the visual observations of the glow pattern. The first is that high pressure tends to contain the glow discharge within the interelectrode volume. The second is that the use of magnets has little obvious effect on the glow pattern except at low pressures and high powers.

The limiting effect of high pressure on the extent of the glow discharge is most evident at low powers where a glow discharge is obtained in only part of the interelectrode volume. The effect is shown in Figure 2 for a flow rate of  $99 \text{ cm}^3$  (S.T.P.)/min at a  $p_M$  of 500 mTorr. Here, the partial glow obtained with 100-W rf power is depicted. As the power is increased to 300 W, there is a transition to full glow, but the glow is weak in the center of the interelectrode volume. Even glow is obtained at 350-W power.

The extent of glow and  $(p_M - p_g)$  are plotted against power for the case of  $F = 9.9 \text{ cm}^3$  (S.T.P.)/min,  $p_M = 500 \text{ mTorr}$ , no magnets, in Figure 3. As would

TABLE I  
 Characteristics of Visually Observed Glow Discharge

Flow Rate, cm <sup>3</sup> (S.T.P.)/min	Magnets	Power W	$P_M$ , (mTorr)	$P_g$ , (mTorr)	Description of glow	$W/FM$ , (J/kg) $\times 10^{-8}$	$W/p_g$ , W/mTorr
1	no	30	25	10	1	4.02	3.0
1	no	100	25	11.5	1+	13.4	8.7
1	MAG	30	25	16	1	4.02	1.9
1	MAG	100	25	15	1	13.4	6.7
1	no	30	300	130	1	4.02	0.23
1	no	100	300	115	1	13.4	0.87
1	MAG	30	300	119	1	4.02	0.25
1	MAG	100	300	122	1	13.4	0.82
2	no	30	40	22	1	2.01	1.4
2	no	100	40	21.5	1+	6.70	4.7
2	MAG	30	40	25	1	2.01	1.2
2	MAG	100	40	26	1	6.70	3.9
2	no	30	300	130	1	2.01	0.21
2	no	100	300	130	1	6.70	0.76
2	MAG	30	300	143	1	2.01	0.21
2	MAG	100	300	132	1	6.70	0.76
9.9	no	30	106	80	1	0.406	0.38
9.9	MAG	30	106	66	1	0.406	0.46
9.9	no	30	300	210	1/2	0.406	0.14
9.9	MAG	30	300	190	1/2	0.406	0.16
9.9	no	30	500	333	1/5	0.406	0.09
9.9	MAG	30	500	332	1/4	0.406	0.09
9.9	no	50	500	333	2/3-	0.677	0.15
9.9	no	60	500	307	3/4	0.812	0.20
9.9	no	70	500	310	3/4+	0.947	0.23
9.9	no	80	500	313	4/5	1.08	0.26
9.9	no	90	500	312	4/5+	1.22	0.29
9.9	no	100	500	313	1	1.35	0.32
9.9	MAG	100	500	288	1/3	1.35	0.35
9.9	no	150	500	271	1	2.03	0.55
9.9	MAG	150	500	280	1-	2.03	0.54
9.9	no	200	500	267	1	2.71	0.75
9.9	MAG	200	500	274	1	2.71	0.73
9.9	no	300	500	260	1	4.06	1.15
9.9	MAG	300	500	270	1	4.06	1.11
99	no	30	500	480	1/4	0.041	0.063
99	MAG	30	500	480	1/4	0.041	0.060
99	no	100	500	460	1/3-1/2	0.135	0.22
99	MAG	100	500	470	1/3	0.135	0.21
99	no	200	500	450	1 <sup>a</sup>	0.271	0.44
99	no	250	500	440	1	0.338	0.57
99	no	300	500	420	1	0.406	0.71
99	MAG	300	500	410	1-	0.406	0.73
99	no	350	500	415	1	0.474	0.84
99	MAG	350	500		1	0.474	

<sup>a</sup> Partial glow at initiation of glow discharge expands to full glow as steady-state condition.



Fig. 2. Partial glow obtained with a flow rate of  $99 \text{ cm}^3$  (S.T.P.)/min,  $p_M = 500 \text{ mTorr}$ , 100-W power, and magnetic enhancement.

be expected  $p_M - p_g$  increases as the extent of glow increases, indicating that there is a more complete polymerization of tetrafluoroethylene at the higher power.

The extent of glow at 30-W power is plotted versus  $p_g$  in Figure 4 for the case of no magnets and in Figure 5 for magnetic enhancement. The glow fills less than the entire volume of the interelectrode gap at values of  $p_g$  above 150–175 mTorr. The extent of glow does not depend uniquely on  $p_M$  (e.g., at  $p_M = 300 \text{ mTorr}$ , extent of glow = 1 or 0.5, depending on flow rate) or on  $F$  (at  $F = 9.9 \text{ cm}^3$  (S.T.P.)/min, extent of glow = 1, 0.5, or 0.2, depending on  $p_M$ ). The dependence of extent of glow on  $p_g$  is practically identical either with or without magnetic enhancement.

Magnetic enhancement has little effect on the appearance of the glow discharge at high pressures, or at low pressures and low power. Upon increasing power the glow appears as shown in Figures 6 and 7. The glow expands out of the interelectrode volume without magnets but is contained within the interelectrode volume close to the electrodes when magnets are used. The most intense glow is found in two diffuse rings concentric with the electrode center axis.

### Deposition Rates

A preliminary survey was run at two different conditions, namely,  $F = 2 \text{ cm}^3$  (S.T.P.)/min,  $p_M = 40 \text{ mTorr}$  at 30-W power; and  $F = 99 \text{ cm}^3$  (S.T.P.)/min,  $p_M = 500 \text{ mTorr}$  at 300 W. The results indicated that deposition rates are fairly similar at the electrode and substrate for the low values of flow rate, initial pressure, and power. The second set of conditions with the increased values of flow rate, pressure, and power gave a tenfold increase in deposition at the elec-

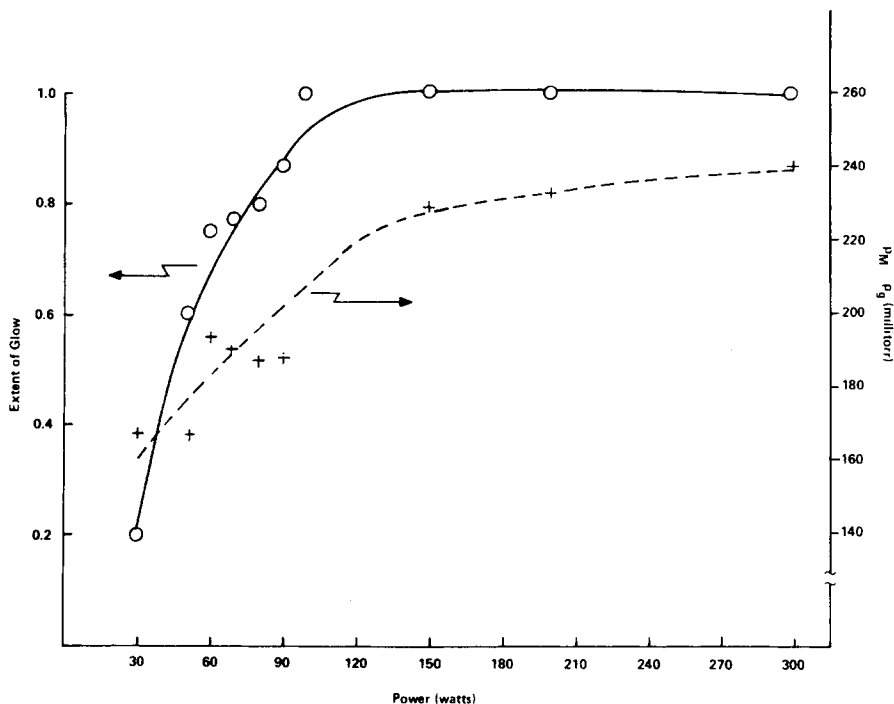


Fig. 3. Extent of glow and  $p_M - p_g$  as function of power with flow rate of  $9.9 \text{ cm}^3$  (S.T.P.)/min,  $p_M = 500 \text{ mTorr}$ , and no magnets.

trode but less than twofold midway between electrodes. As the deposition rate midway between electrodes is the one of practical interest, it is clear that very little is gained by polymerizing at high flow rate, power and pressure. In fact, the heat generated between electrodes is so high in this case that a Mylar substrate, encased in aluminum and placed between the electrodes, melted when polymerization was attempted. (This was attempted only without magnetic enhancement). For these reasons no further work was done in glow discharges at the higher flow rate, pressure, and power combination.

Deposition rate data were collected (for glow discharges run at  $F = 2 \text{ cm}^3$  (S.T.P.)/min,  $p_M = 60 \text{ mTorr}$ ) as a function of distance from the electrodes center axis both on the electrode and on the substrate. These data are presented in Figure 8 for plasma generated at three power levels without magnets. The highest electrode deposition rate is at the intermediate power level. The substrate deposition rate decreases with increasing power. The corresponding data for magnetically enhanced plasma is presented in Figure 9. Conversions of TFE to plasma are presented in Table II. These represent the total deposition on both surfaces of a 6-cm-radius electrode or on a comparable surface area on the substrate. This total deposition rate is divided by the monomer flow rate expressed as mass/unit time. Magnetic enhancement tends to increase the deposition rate at the electrode and at the substrate at 30 and 100 W. However, the highest deposition rate at the substrate is obtained at 10-W power without magnets. This has the further advantage of being fairly evenly distributed over the substrate surface. Figure 10 is a plot of the ratio of the substrate to electrode



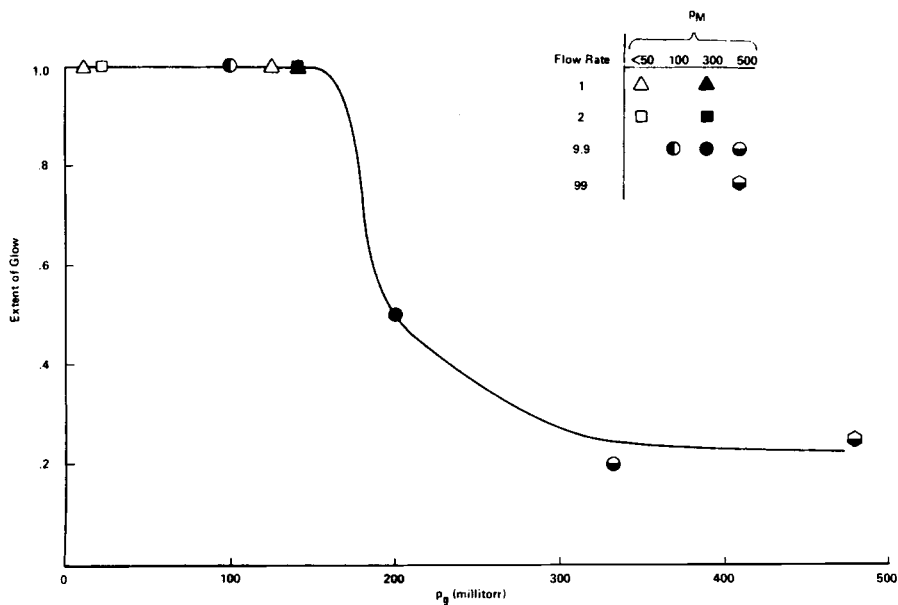


Fig. 4. Extent of glow at 30-W power as function of  $p_g$  without magnets.

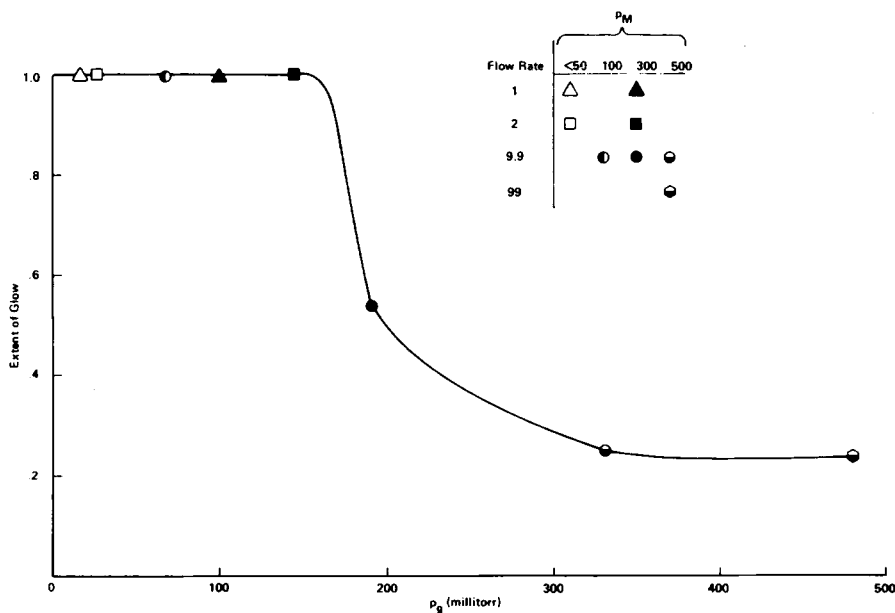


Fig. 5. Extent of glow at 30-W power as function of  $p_g$  with magnetic enhancement.

conversion as a function of power. The drop with increasing power is considerably more precipitous without magnets than for the magnetically enhanced case.

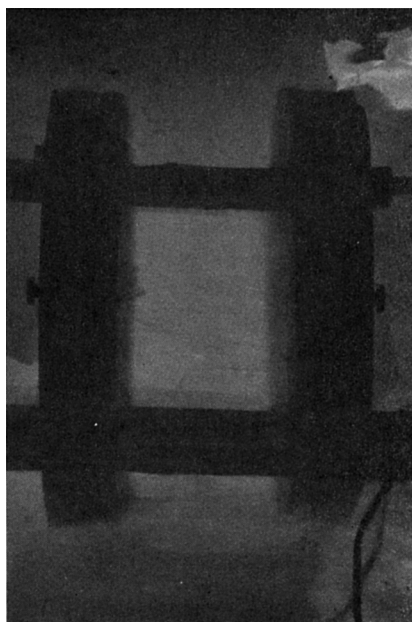


Fig. 6. Glow discharge obtained using a flow rate of  $2 \text{ cm}^3$  (S.T.P.)/min,  $p_M = 40 \text{ mTorr}$ , 100-W power, and no magnets.

TABLE II  
Conversion of TFE to Polymer at a Flow Rate of  $2 \text{ cm}^3$  (S.T.P.)/min,  $p_m = 60 \text{ mTorr}$

Magnets	Power, W	$W/FM$ , (J/kg) $\times 10^{-8}$	$p_g$ , mTorr	TFE Conversion to plasma polymer	
				Electrode, %	Substrate, %
no	10	0.67	38	6.2	4.7
no	30	2.01	36	8.9	2.0
no	100	6.70	34	5.2	.03
MAG	10	0.67	37	8.6	1.5
MAG	30	2.01	36.5	11.0	3.3
MAG	100	6.70	36	7.4	0.7

### Pressure in the Glow Discharge

A comparison of the pressure during the glow discharge with that obtained before plasma initiation is an indication of the relative importance of depletion of the gaseous phase by polymerization as opposed to an increase in the number of gaseous species caused by abstraction of fluorine atoms from the monomer. In inductively coupled plasmas the inception of a plateau in a  $p_g$  (pressure in plasma)-versus-power plot has been used to indicate the inception of "full glow" conditions.<sup>10</sup> Plots of  $p_g$  versus power are presented for the no-magnet case in Figure 11 and for a magnetically enhanced plasma in Figure 12. A plateau is achieved at the lowest applied power (5 W) in the latter case, but only at about 60 W without magnets.



Fig. 7. Glow discharge obtained using a flow rate of  $2 \text{ cm}^3$  (S.T.P.)/min,  $p_M = 40 \text{ mTorr}$ , 100-W power, and magnetic enhancement.

### ESCA Spectra

ESCA results were obtained for a flow rate of  $2 \text{ cm}^3$ (S.T.P.)/min at  $p_M = 60 \text{ mTorr}$  at 10- and 100-W power. As shown in Table III, samples of polymer deposited on the electrode and substrate on the electrode center axis were taken both with and without magnetic enhancement. For magnetic enhancement additional samples were obtained at a radius of 4 cm (the location of an intense annular glow).

As shown in Figures 13–16, the  $C_{1s}$  spectra demonstrate varying amounts of fluorine bound to carbon. The  $C_{1s}$  spectra shown in Figures 13 and 14 for 0E 10N rf (key to this notation is at foot of Table III) and 0E 100N rf, respectively, have peaks at 293.5 eV ( $CF_3$ ), 292. eV ( $CF_2$ ), and the peak at 284.6 eV attributed to hydrocarbon or graphitic carbons. The peaks between 291. eV and 284.6 eV are attributed to carbons bound to one fluorine atom or other electronegative species (e.g., O or N). The spectra shown in Figures 15 and 16 for 0S 100N rf and 0E 100MAG rf, respectively, show much less prominent peaks indicative of carbons bound to fluorine and a very prominent carbon peak at 284.6 eV. An obvious qualitative numerical indicator of these characteristic peak shapes is the ratio of the peak height at 291.5 eV ( $CF_2$ ) to that at 284.6 eV. This ratio is given in the last column of Table III.

The F/C elemental ratio is generally a constant, regardless of plasma polymerization conditions. However, for samples prepared with magnetic enhancement and 100 watts power, the peak height ratio in the last column is so low that some of the fluorine reported may be bound to sputtered aluminum. Low  $C_{1s}$  291.5 eV to 284.6 eV ratios are, in all cases, accompanied by high O/C ratios and the presence of aluminum on the surface of the sample.

It appears that some of the oxygen detected may also be bound to aluminum.

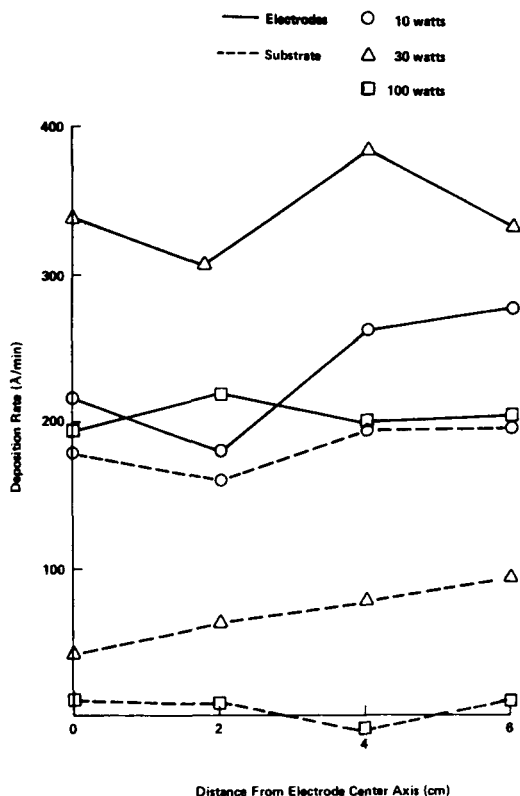


Fig. 8. Deposition rate profile on electrodes and substrate for a rf plasma at a flow rate of  $2 \text{ cm}^3$  (S.T.P.)/min,  $p_M = 60 \text{ mTorr}$ , and no magnets.

Low O/C ratios in Table III are accompanied by oxygen peak positions of 533 to 535 eV indicative of covalently bound oxygen. However, when the reported O/C ratio exceeds 0.75, the oxygen peak position is below 531.5 eV, indicating that at least some of the reported oxygen is from oxygen bound to aluminum on the surface.

The results obtained at 100 W without magnets are particularly unusual. The spectra obtained for the electrode sample show the presence of a considerable population of  $\text{CF}_2$  and  $\text{CF}_3$  groups with a low O/C ratio and no detectable aluminum, in short, spectra typical of all the 10-W samples. The substrate ESCA spectra are distinctly different and are similar to those obtained for the 100-W, magnetically enhanced samples.

## DISCUSSION

### High-Pressure Plasma

The TFE plasma is of great interest in the effort to understand how the deposition of plasma polymer and chemical nature of that polymer are affected by the variables at our disposal. These include the feed rate of monomer into the reactor, the pumping rate (out of the reactor) applied to gaseous products

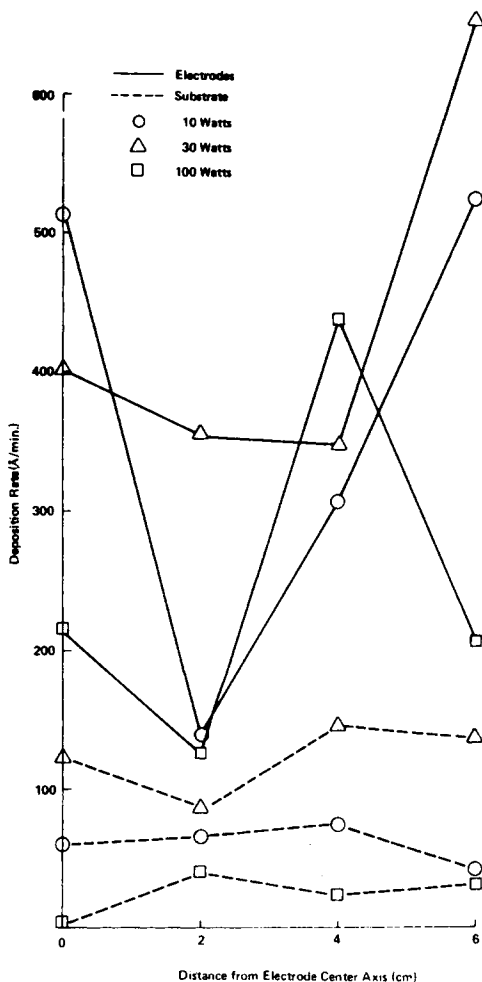


Fig. 9. Deposition rate profile on electrodes and substrate for a rf plasma at a flow rate of  $2 \text{ cm}^3$  (S.T.P.)/min,  $p_M = 60 \text{ mTorr}$ , and with magnetic enhancement.

of plasma and residual monomer (if any), and the power fed into the plasma. The relationships between these variables that allow maximum conversion of monomer to plasma polymer in an inductively coupled system appear to be applicable in a capacitively coupled system as well.

For example, in our standard inductively coupled system (see Introduction) it has generally been found that a plot of pressure or of deposition rate versus power will reach a plateau at power levels which allow the reactor volume to be completely filled with glow. A composite parameter that describes the energy provided per gram of monomer feed is  $W/FM$ . For a given monomer, the quantity  $W/FM$  must exceed  $W_c/FM$  in order for the "full glow" condition to be realized.<sup>10</sup> An analogous phenomenon has been observed in the capacitively coupled TFE plasma described here. Only a portion of the interelectrode gap contains glow at low values of  $W/FM$ . Under such conditions, less polymerization occurs than in the full glow state as shown in Figure 3. Plasma poly-

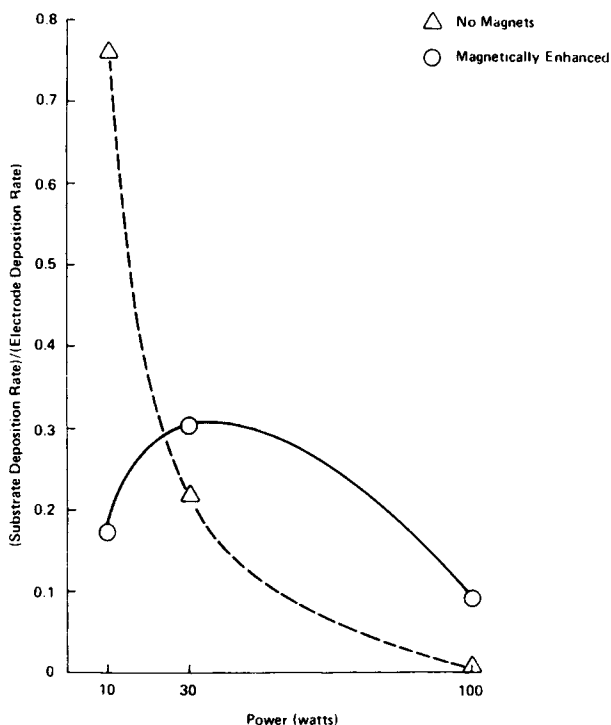


Fig. 10. Ratio of substrate to electrode integrated deposition rate as a function of power. Flow rate is  $2 \text{ cm}^3$  (S.T.P.)/min and  $p_M = 60 \text{ mTorr}$ .

merization removes monomer molecules from the gas phase and yields new gas molecules when atoms are abstracted from monomer or polymer molecules. When the number of molecules removed from the gas phase exceeds the number formed, the pressure in a flow system decreases on inception of the glow discharge. The quantity  $p_M - p_g$  describes this decrease and is a measure of the relative amount of polymer deposition. As seen in Figure 3, both the extent of glow and  $p_M - p_g$  reach a plateau (actually a very low slope for  $p_M - p_g$ ) above  $150 \text{ W}$  ( $W/FM = 2 \times 10^8 \text{ J/kg}$ ). For comparison,  $W_c/FM$  is found to exceed  $1.2 \times 10^8 \text{ J/kg}$  for our inductively coupled system.

However, in evaluating  $W/FM$  data obtained for such a capacitively coupled system, it should be remembered that the flow rate of monomer into the glow zone is not precisely known. In this paper we have taken  $F$  as the flow rate into the reactor volume as the best approximation available of the somewhat smaller flow rate into the glow discharge (between electrodes). Because of this the actual energy available per gram of monomer would tend to be higher than our nominal  $W/FM$  values. The nominal  $W/FM$  values are therefore a lower limit to the actual  $W/FM$ .

On the other hand, not all power delivered to the glow discharge is available for plasma polymerization. Some of it must be used to excite product gas. This contribution increases, for a given feed rate, as the pumping rate is decreased. A measure of the power per molecule available for this purpose is  $W/p_g$ . The importance of this latter parameter is shown in Figure 4 where it is seen that when the power applied is kept at  $30 \text{ W}$ , the extent of glow is determined by  $p_g$ . In

TABLE III  
Summary of ESCA Data for Plasma Polymer of Tetrafluoroethylene Deposited in a Capacitively Coupled rf Glow Discharge ( $F = 2 \text{ cm}^3 \text{ (S.T.P.)/min}$ ,  $P_M = 60 \text{ mTorr}$ )

Code <sup>a</sup>	Peak area corrected for photoelectric cross section, (counts eV) $\times 10^{-4}$			Oxygen peak position, (eV)	Elemental ratio			Peak height ratio	
	O <sub>1s</sub>	F <sub>1s</sub>	C <sub>1s</sub>		Al <sub>2s</sub>	O/C	F/C	Al/C	C <sub>1s</sub> 291.5 eV/ C <sub>1s</sub> 284.6 eV
0E 10N rf	.047	3.38	2.08	0	534.4	0.022	1.63	0	2.44
0S 10N rf	.062	4.83	3.08	0	533.4	0.020	1.57	0	2.05
0E 100N rf	.040	3.71	2.07	0	534.5	0.019	1.79	0	3.57
0S 100N rf	1.25	2.58	1.53	1.20	531.4	0.82	1.69	0.78	0.15
0E 10MAG rf	.082	3.24	2.08	0	534.7	0.039	1.56	0	2.27
4E 10MAG rf	.052	3.50	2.07	0	535	0.025	1.86	0	3.70
0S 10MAG rf	.078	5.16	3.16	0	533.2	0.025	1.63	0	2.86
4S 10MAG rf	.065	5.22	3.14	0	533.4	0.021	1.66	0	2.86
0E 100MAG rf	0.51	1.99	1.11	1.36	532.5	0.46	1.79	1.23	0.035
4E 100MAG rf	0.73	1.33	1.06	0.88	531.9	0.69	1.25	.83	0.026
0S 100MAG rf	1.39	2.26	1.30	1.25	531.4	1.07	1.74	0.96	0.038
4S 100MAG rf	1.16	2.34	1.39	1.27	531.1	0.83	1.68	0.91	0.039

<sup>a</sup> OE 10N rf indicates a sample taken 0 cm from the center of the electrode at 10 watts power using no magnets and rf power. 4S 100MAG rf indicates a sample taken 4 cm from the electrode center axis on the substrate at 100-W power using magnetic enhancement and rf power.

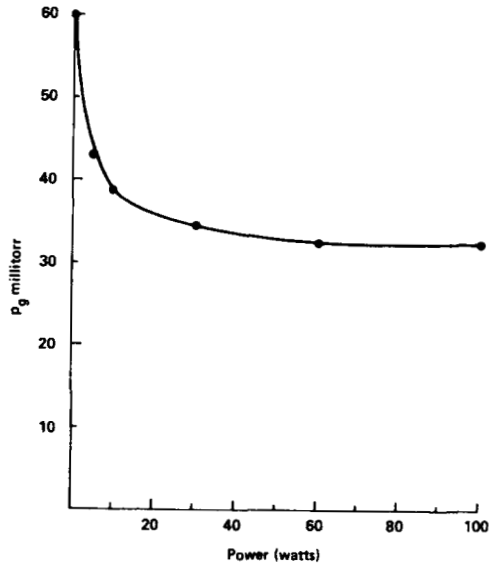


Fig. 11. Plot of  $p_g$  vs power at a flow rate of  $2 \text{ cm}^3$  (S.T.P.)/min,  $p_M = 60 \text{ mTorr}$ , and no magnets.

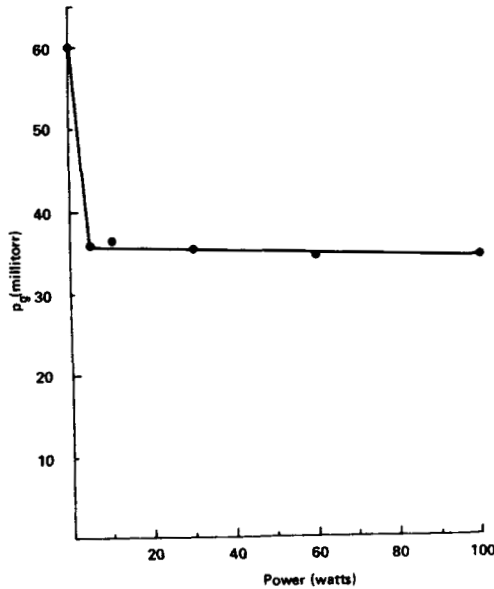


Fig. 12. Plot of  $p_g$  vs power at a flow rate of  $2 \text{ cm}^3$  (S.T.P.)/min,  $p_M = 60 \text{ mTorr}$ , with magnetic enhancement.

this case the  $W/FM$  value is the same for all three points representing a flow rate of  $9.9 \text{ cm}^3/\text{min}$ , i.e.,  $0.41 \times 10^{-8} \text{ J/kg}$ . However, by decreasing the pumping rate, the extent of glow is decreased from 1 to approximately  $1/4$ . The generalization



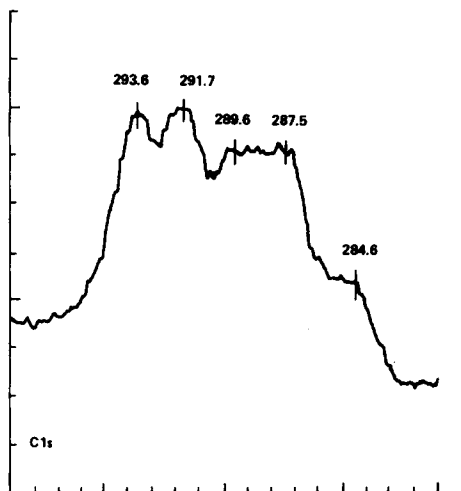


Fig. 13.  $C_{1s}$  spectrum of plasma deposited on the electrode center with a flow rate of  $2 \text{ cm}^3$  (S.T.P.)/min,  $p_M = 60 \text{ mTorr}$ , 10-W power, and no magnets.

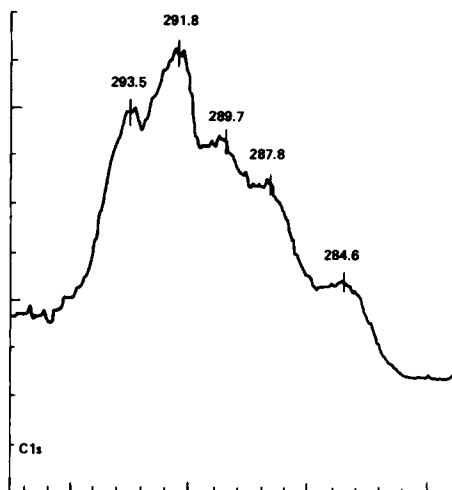


Fig. 14.  $C_{1s}$  spectrum of plasma deposited on the electrode center with a flow rate of  $2 \text{ cm}^3$  (S.T.P.)/min,  $p_M = 60 \text{ mTorr}$ , 100-W power, and no magnets.

that appears to fit all the data, obtained without magnets, in Table I is that if  $W/FM$  is below  $1 \times 10^{-8} \text{ J/kg}$  and  $W/p_g$  is below  $0.3 \text{ W/mTorr}$ , the glow will not fill all of the interelectrode volume.

The high-pressure data also revealed that magnets have a subtle but discernible effect on the plasma polymerization. On the one hand, the visual appearance of the glow discharge is not affected by magnets, and Figures 4 and 5 are identical. On the other, examination of Table I does reveal that a given volume of glow is more efficient in effecting polymerization when magnets are used. For example, for flow rates of 9.9 and  $99 \text{ cm}^3/\text{min}$ , "full glow" is achieved at lower powers for the no-magnet case than with magnets while  $p_g$  of the two cases are approximately equal at equal powers or smaller for the with-magnet case. This may be caused by the helical path that electrons must traverse when magnets are present thus producing more excited molecules per unit volume. More power

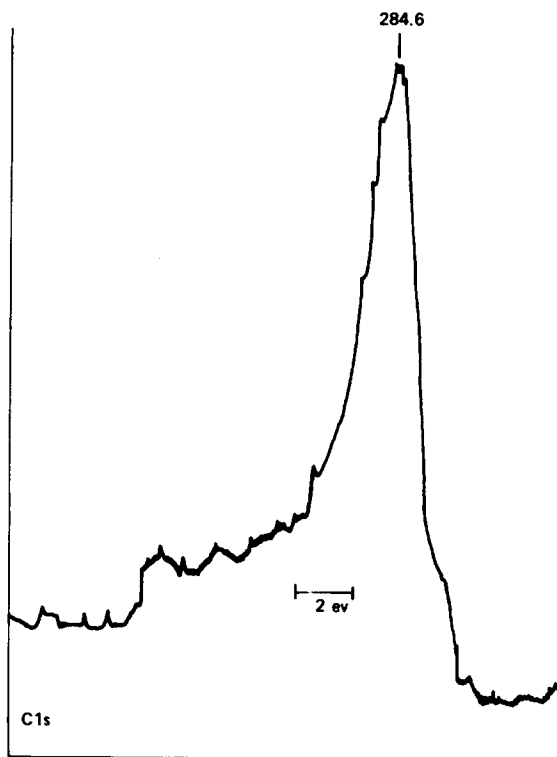


Fig. 15.  $C_{1s}$  spectrum of plasma deposited on the substrate at the intersection with the electrode center axis, with a flow rate of  $2 \text{ cm}^3$  (S.T.P.)/min,  $p_M = 6 \text{ mTorr}$ , 100-W power, and no magnets.

is therefore lost to a given volume of plasma when magnets are used. For this reason more power must be applied to achieve full glow with magnets.

Regardless of whether magnets are present or not, the glow filling a fraction of the interelectrode volume always hugs one edge of the electrodes (See Fig. 2). It never fills the middle only. The middle of the volume is filled only after glow has been attained at the entire circumference. This may be related to the high electric field present at surfaces of a high degree of curvature (sharp points). Thus, conditions may be more favorable for the formation of a glow discharge at the relatively sharp edges of the electrodes when power is low.

### Low-Pressure Plasma

Full glow was achieved for all low-pressure plasma experiments. The data provide a clear picture of the distribution of power in the interelectrode gap and of changes in this distribution with increasing total power input. The results for the magnetically enhanced case and the no-magnet case are discussed separately.

#### *No Magnets*

Deposition rate data can be interpreted on the basis of the known behavior of a TFE glow discharge as a function of power. In an inductively coupled system,<sup>1</sup> the deposition rate was seen to increase with increasing power, reach a

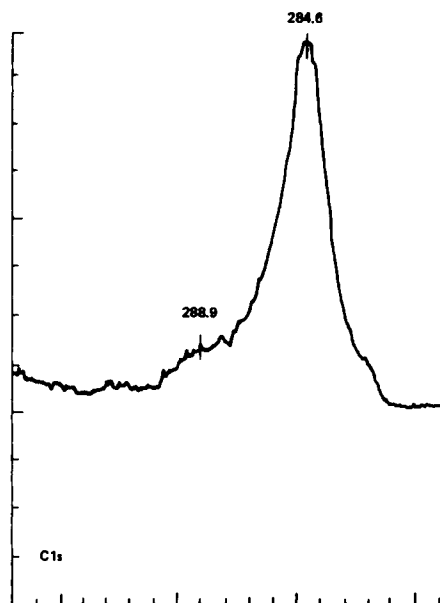


Fig 16.  $C_{1s}$  spectrum of plasma deposited on the electrode center axis with a flow rate of  $2 \text{ cm}^3$  (S.T.P.)/min,  $p_M = 6 \text{ mTorr}$ , 100-W power, with magnetic enhancement.

plateau, and then decrease at very high power levels. A low deposition rate may therefore indicate either a very low or a very high power density. ESCA data can distinguish between these two alternatives because the low deposition rate at high-power levels is due to carbon-fluorine bond breakage resulting in a fluorine poor polymer.

The known physics of rf plasmas employing internal electrodes is also relevant. The mechanism by which electrons pick up sufficient energy from the rf field involves random collisions of electrons with gas atoms, the electron picking up an increment of energy with each collision.<sup>14</sup> It follows that a volume in which electrons are not able to participate in a sufficient number of oscillations to reach ionizing energy will be a volume of low reactivity. Such a volume element is found at and near the electrodes where electrons are drawn from the plasma during the positive half of the rf cycle. Both electrodes therefore develop a negative bias with respect to the glow discharge, with the result that cations drift toward the electrodes. The size of the relatively inactive zone next to the electrode is proportional to the electric field and to the electron mobility. It therefore increases with increasing power and decreasing pressure. In fact, at high power and low pressure an rf glow discharge is observed to spread outside the interelectrode volume so that a glow is observed surrounding the set of electrodes while the interelectrode volume itself remains relatively dark. The first stages in this process are seen in Figure 6.

The deposition rate data shown in Figure 8 and Table II depict a deposition rate at the substrate that decreases with increasing power over the power range of 10–100 W. This corresponds to a  $W/FM$  range of  $6.7 \times 10^7$  to  $6.7 \times 10^8 \text{ J/kg}$ . A decrease in deposition rate at the electrode with increasing power is only observed between 30 and 100 W. Moreover, ESCA (Table III) reveals that the polymer formed at the electrode is fluorine rich. The decrease in electrode de-

position rate when power is *increased* to 100 W is apparently caused by a *decreased* power density at the electrode. As explained above, a relatively inactive zone close to the electrodes, caused by extraction of electrons from the plasma, expands with increasing power. Thus, power is concentrated midway between electrodes and at power levels just below those at which the plasma expands out of the interelectrode gap the power density observed is very high in the center of the gap and very low at the electrode. This is indicated by the  $C_{1s}$  spectra shown in Figures 14 and 15 and the ESCA data given in Table III. It may be noted that the F/C ratio and peak height ratio for the 0E 100N rf sample are among the highest in the table.

When compared to the results obtained for an inductively coupled straight-tube reactor, it is found that the total conversions obtained with the capacitively coupled reactor are somewhat lower. Conversions of 10–20% are estimated for the inductively coupled reactor.<sup>2</sup> On the other hand, higher F/C and peak height ratios are obtained (at lower power) from the ESCA data in this work than were observed for the inductively coupled samples. Particularly striking is the near-constancy of the F/C ratio in Table III, whereas it decreased at high power for the inductively coupled case. This may be related to a more efficient pumping out of gaseous by-products (fluorine) in the inductively coupled case.

The evidence that fluorine is bonded to aluminum as well as carbon for those cases where a fluorine-poor polymer is formed and the concomitant presence of oxygen in the polymer, as revealed by ESCA, were observed for the inductively coupled case as they are here. The oxygen is most probably incorporated in the polymer by reaction of polymeric free radicals with oxygen after the plasma polymer is exposed to air.

#### *Low-Pressure Plasma with Magnetic Enhancement*

The use of magnets prevents escape of electrons from the interelectrode gap and concentrates the glow discharge closer to the electrodes as shown in Figure 7. As seen in Figure 9, the deposition rate distribution is very uneven over the electrode surface but markedly less so over the substrate surface. The hypothesis that an energy-poor zone existed near the electrodes without magnets is further supported by the increase in conversion at the electrode (see Table II), observed at all power levels when magnetic enhancement is employed.

ESCA reveals that a low-power environment is experienced at all points at 10 W. The exceptionally high peak height ratio and F/C elemental ratio seen for 4E 10MAG RF may be noted, akin to that seen for 0E 100 N RF. There is no obvious explanation for this, but the sample is close to the intense glow discharge ring observed when magnetic enhancement is employed.

The more efficient use of power with magnetic enhancement is noted at 100 W in two observations. Firstly, all samples (not only those at the substrate) show the typical high aluminum- and oxygen-containing surface expected at high power. Secondly, the peak height ratios for all 100-W, magnetically enhanced samples are smaller than that seen for 0S 100N RF, indicating less  $CF_3$  and  $CF_2$  groups in the plasma polymer formed with magnets than without at all locations (compare also Figs. 15 and 16). Electrons achieve energies required for ionization or free-radical formation only after a number of random collisions.<sup>14</sup> Electrons

that leave the plasma after only a few collisions have therefore absorbed energy without contributing to the plasma polymerization (or fluorine abstraction) process. Since magnetic enhancement prevents loss of electrons from the reactive zone, this energy loss is prevented, and a greater efficiency in converting energy input to plasma polymerization (or fluorine abstraction) results.

The more even distribution of power between substrate and electrode is seen dramatically in the ratio of substrate to electrode conversion ratio shown in Figure 10. The sharp drop when magnets are not used is caused by the projection of power almost exclusively to the center of the electrode gap, particularly at high powers. This is prevented when magnetic enhancement is employed, as is the expansion of the glow outside the interelectrode gap. This makes a greater range of powers and  $W/FM$  values practical.

Finally, the more efficient use of rf power with magnetic enhancement is demonstrated by the onset of a plateau in the  $p_g$ -versus-power plot of Figure 12 at the lowest power employed, 5 W, whereas such a plateau is only attained at about 60 W when magnets are not used (see Fig. 11). It may also be noted that conversions are increased by the use of magnetic enhancement so as to be comparable to those observed for an inductively coupled straight tube reactor.

The comments made in comparing ESCA spectra for the no-magnet case with those for inductively coupled plasma polymer are applicable for the magnetically enhanced case as well. The presence of aluminum in the low fluorine-containing plasma polymer samples indicates a competitive plasma polymer deposition and ablation that occurs in the presence of energetic fluorine ions. Scanning electron micrographs of ESCA samples prepared at 100 W with magnetic enhancement reveal the same surface as for an aluminum blank not coated with plasma polymer and for an aluminum blank covered with TFE plasma polymer at low power such that no aluminum appears in the ESCA data. Thus, the presence of aluminum does not indicate powder formation but simply a competitive deposition-ablation that may leave some parts of the surface not covered or that sputter aluminum atoms onto the surface.

## CONCLUSIONS

1. At low values of  $W/FM$  and high pressures a glow discharge covering only a portion of the interelectrode gap may be obtained. To obtain a discharge filling the entire volume, both  $W/FM$  and  $W/p_g$  must exceed certain limits.
2. Deposition rate and ESCA data for low flow-rate, low-pressure plasmas can be interpreted on the basis of a model in which power is coupled to the center of the interelectrode gap to a greater extent than the immediate vicinity of the electrodes, in the absence of a magnetic field. With magnetic enhancement, the region of high power density moves closer to the electrodes.
3. The use of magnets leads to a more efficient coupling of energy input to plasma polymerization and/or reaction under all sets of conditions examined. The effects are subtle at high pressure but more obvious for the combination of low pressure, flow rate, and high power.

The authors gratefully acknowledge the experimental contributions of Barry Hill who prepared all plasma polymers described and collected all experimental data with the exception of the ESCA spectra. This work was supported by the Office of Water Research and Technology of the U.S. Department of the Interior under Contract Nos. 14-30-3301 and 14-34-0001-7537. Two of us, E.S.B.

and C.N.R., are grateful for funding supplied during the period of this study from the National Science Foundation.

### References

1. H. Yasuda, T. S. Hsu, E. S. Brandt, and C. N. Reilley, *J. Polym. Sci., Polym. Chem. Ed.*, **16**, 415 (1978).
2. H. Yasuda, N. Morosoff, E. S. Brandt, and C. N. Reilley, *J. Appl. Polym. Sci.*, **23**, 1003 (1979).
3. D. F. O'Kane and D. W. Rice, *J. Macromol. Sci., Chem. A* **10**, 567 (1976).
4. D. W. Rice and D. F. O'Kane, *J. Electrochem. Soc.*, **123**, 1308 (1976).
5. B. D. Washo, *J. Macromol. Sci., Chem. A* **10**, 559 (1976).
6. M. M. Millard and A. E. Pavlath, *J. Macromol. Sci., Chem. A* **10**, 579 (1976).
7. F. Biederman, S. M. Ojha, and L. Holland, *Thin Solid Films*, **41**, 329 (1977).
8. H. Yasuda and C. E. Lamaze, *J. Appl. Polym. Sci.*, **17**, 1519 (1973).
9. H. Yasuda and T. Hirotsu, *J. Polym. Sci., Polym. Chem. Ed.*, **16**, 313 (1978).
10. H. Yasuda and T. Hirotsu, *J. Polym. Sci., Polym. Chem. Ed.*, **16**, 743 (1978).
11. N. Morosoff, H. Yasuda, E. S. Brandt, and C. N. Reilley, *J. Appl. Polym. Sci.*, **23**, 3471 (1979).
12. N. Morosoff, W. Newton, and H. Yasuda, *J. Vac. Sci. Tech.*, **15**, 1815 (1978).
13. H. Yasuda, H. C. Marsh, E. S. Brandt, and C. N. Reilley, *J. Polym. Sci., Polym. Chem. Ed.*, **15**, 991 (1977).
14. L. Maissel, in *Handbook of Thin Film Technology*, L. I. Maissel and R. Glang, Eds., McGraw Hill, New York, 1970.

Received June 19, 1978

Revised August 18, 1978